Deep Mining 2024 – P Andrieux & D Cumming-Potvin (eds)

doi:10.36487/ACG_repo/2465_47

Numerical model calibration of fault properties using seismic moment for a deep underground mine

Cinthia Maldonado [a,*], Tatyana Katsaga [a], Hao Li [a]

[a] *ITASCA, Canada*

Abstract

Microseismicity often provides crucial insights into the behaviour of rock masses in deep mining environments, especially concerning damage and the mechanisms affected by stress field changes. By integrating numerical simulations of synthetic microseismicity with field data analysis, a comprehensive understanding of damage initiation, progression, and the interactions among discontinuities can be attained. This holistic approach not only advances our comprehension of rock mass behaviour in deep mining operations but also enables more precise predictions and proactive management strategies to mitigate risks.

This study delves into the methodology employed for calibrating numerical models, focusing on the geological structures within a deep mine in Canada. The occurrence of significant seismic events in this deep mine is directly linked to fault slip. With mining operations delving deeper, understanding the stress-induced effects of mining and fault movements becomes paramount for ensuring safe ore extraction.

Merely incorporating lithological considerations into the numerical model proved to be insufficient to replicate the full behaviour of the rock mass response to seismic activity. Hence, fault structures were integrated into the model. However, due to the volumetric nature of faults with a thickness exceeding 1.5 m, explicit integration was deemed inadequate for accurately representing their behaviour. To address this challenge, a methodology termed the 'weak zone' approach was developed. With this approach, faults are characterised as relatively weaker materials compared to the host rock, and the cumulative plastic shear strain is utilised for calculating seismic moment.

Historically recorded seismicity served as a crucial calibration tool for determining the mechanical properties of faults within the model. These properties were then appropriately scaled to ensure that the modelled results provided a reasonable estimation of fault behaviours in relation to seismic moment. This comprehensive approach not only enhances our understanding of fault dynamics in deep mining environments but also aids in optimising safety measures for ore extraction.

Keywords: *fault behaviour, fault slip, seismicity, seismic moment, numerical model calibration*

1 Introduction

Advancing our understanding of rock mass behaviour in different stress environments is challenging but essential for successful mining operations. Rock mass behaviour is governed by the behaviour of the intact material and discontinuities, which include veins, joints, faults, and other geological features. Mining operations induce stress changes, causing fracturing of the intact material and reactivation of the discontinuities. Fracturing and slip on existing structures release energy that can be recorded as microseismic events and studied to provide answers to fundamental questions. Recent advances in microseismic monitoring and advanced data processing provide valuable information about in situ rock mass behaviour in terms of damage when subject to changes in the stress field. Numerical investigations of simulated synthetic

* Corresponding author. Email address: cmaldonado@itasca.ca

microseismicity along with field data can provide valuable insight into the details of damage initiation, development, and discontinuity interaction (Basson et al. 2021; Blanksma et al. 2022, Katsaga & Pierce 2013).

In deep mines, stress hazards such as large seismic events pose potential risks to mining operations due to high stress (Andrieux et al. 2004) in both the rock mass and the fault slip. The mine's engineers possess extensive expertise in managing high stresses in such a deep environment. They implement best practices to uphold profitability while prioritising worker health and safety. To sustain these efforts, the mine employs one of the mining industry's most expansive microseismic arrays. Since 1980, they have been actively monitoring microseismic responses to mining activities. Recorded microseismicity was used successfully for advanced interpretations (e.g. Mercer & Bawden 2005; Cotesta et al. 2014).

At this mine, analysis of monitored historical seismic events indicates that major structures may play a key role in causing seismic events due to fault slip-induced shear movement, energy release, and migration of high stress. Many efforts have been made in the past years to quantify seismic moment caused by fault slip through numerical modelling. Salamon (1993) and Board (1996) proposed a methodology for estimating the seismic moment of fault slip using the concept of extra shear stress (ESS) suggested by Ryder (1987, 1988), and Cancino et al. (2019) presented another method of calculation of seismic moment by distinguishing between seismic and aseismic shear displacement based on a criterion of onset of fracture suggested by Martin (1993). The shear displacements are not explicitly simulated in their modelling. Sjoberg et al. (2012) evaluated the potential for fault slip rockbursting by calculating the seismic moment resulting from shear displacements that are explicitly modelled along geological structures using 3DEC; a numerical modelling tool based on the distinct element method.

In the study area of the mine, there are 22 faults mapped and some historical large seismic events recorded were believed to be associated with the slip of some faults. To quantitatively estimate the seismic event triggered by a fault slip mechanism, it is conservatively assumed in this study that the seismic event is caused by the energy release due to the plastic shearing of the fault. A FLAC3D model was used to calculate the plastic shear strain and normal stress of each zone in the fault, and the seismic moment was then obtained by summing up the released energy of each group of connected zones. The detailed procedure of computation is explained in the modelling approach section. The properties of the fault must be calibrated against historical monitoring seismic events before using the model to do any predictive simulation.

2 Modelling approach and implementation

This work is based on FLAC3D (Fast Lagrangian Analysis of Continua in 3 Dimensions; ITASCA 2023) where rock mass behaviour is simulated using a strain softening constitutive model, ITASCA Constitutive Model for Advanced Strain Softening (IMASS), with a Hoek–Brown yield criterion.

2.1 The ITASCA Constitutive Model for Advanced Strain Software

The IMASS model has been developed to represent the rock mass response to excavation-induced stress changes. IMASS models the damage around excavations by accounting for the progressive failure and disintegration of the rock mass. It is based on empirical relationships and uses strain-dependent properties. IMASS is the result of numerous successful engineering consulting projects and research on brittle rock behaviour. This constitutive model was selected for this project due to its powerful features and its ability to closely mimic the behaviour of rock mass under complex induced stresses.

2.2 Modelling approach

Various methods can be employed to introduce faults into the model and estimate the seismic moment caused by fault slip, including:

- Explicit representation of faults: This approach simplifies the fault as a surface along which the host rock on both sides undergoes slip. The stress drop and seismic moment can be modelled at each cycle step using the Mohr–Coulomb constitutive model, typically utilised for simulating shearing

along the fault surface. Mechanical parameters such as cohesion, friction angle, normal and shear modulus need to be estimated and calibrated.

- Weak zone simulated with IMASS: In this method, the fault is represented as a material weaker than the host rock. The accumulated plastic shear strain can be employed to calculate the seismic moment. The mechanical properties of the fault material can be estimated and calibrated based on factors such as brittleness coefficient and downgrading rock mass characteristics, geological strength index (GSI) and uniaxial compressive strength (UCS) to reflect rock mass deterioration.

The approach of simulating a weak zone with IMASS was utilised for fault modelling and calibration in this study due to the following factors:

- The faults have a thickness exceeding 1.5 m, ranging from 1.5 to 300 m. The geometry of these faults is volumetric.
- The rock units within the fault are almost identical to the host rock. Therefore, it is more reasonable to estimate fault properties by scaling down the mechanical properties of the host material.

To calculate the seismic moment generated by the fault through numerical modelling, the seismic moment, M_0, serves as a robust measure of the magnitude of a shear-type seismic event and is defined by the following equation:

$$M_0 = G * A * d \ (M.m) \tag{1}$$

where:

M_0 = seismic moment.

G = shear modulus in pascals.

A = area of the rupture surface in square metres.

d = mean ride or shear displacement in metres.

Additionally, the Richter magnitude (M) of an event can be determined using the following formula:

$$M = \frac{2}{3} log_{10} M_0 - 6.07 \tag{2}$$

where M is Richter magnitude of seismic event.

The method employed in FLAC3D for calculating seismic moment in modelling is as follows:

- Extract and refine the middle surface of each fault, as illustrated in Figure 1, using Delaunay triangulation.
- Perform numerical modelling at each mining step.
- Identify and determine the nearest zone for each node on the fault surface.
- Obtain the accumulated plastic shear strain and normal stress of the nearest zone.
- Calculate the incremental plastic shear strain (ds) during the current time step (mining step) if the normal stress exceeds a predetermined threshold.
- Calculate the shear displacement (d) as the product of ds and the diameter (R) of the connected nodes area.
- Determine the seismic moment of each node using Equations 1 and 2.
- Compute the seismic moment of each fault by summing the calculated seismic moments of the nodes. The total seismic moment should be multiplied by the average thickness of the fault.

Figure 1 The middle surface obtained from the given volumetric geometry of the fault

For each mining step, the seismic moment of each fault was calculated and compared with historical seismic moments. The mechanical properties of each fault were then iteratively adjusted and calibrated to ensure a close match between the modelled seismic moment and the historical values. The following properties of IMASS are adjusted and downscaled to achieve the best match with monitored data:

- GSI: Rock within fault is assumed to be degraded.
- Brittleness coefficient: A parameter of IMASS that controls the brittleness of the rock mass. The value is in the range of 0 to 1. The lower the value is, the more brittle the rock is.
- UCS and Young's modulus: Intact rock is assumed to be changed because of fluid or tectonic movement.

Achieving a good match at every mining step for all the faults is challenging due to the nature of numerical models. Calibration primarily focuses on the following aspects:

- Matching the modelled average seismic moment of each fault with the recorded average value, especially for the most active faults such as Fault 02, Fault 06, Fault 07, Fault 09, Fault 20, Fault 21, and Fault 22.
- Matching the modelled cumulative seismic moment of all faults with the recorded value. The cumulative seismic moment in the mine indicates the potential risk of stress hazards in a global sense and can be utilised to optimise the mining design for future production plans.

Furthermore, the location and magnitude of clustered seismic moments were modelled by grouping adjacent zones that exhibited shearing movement, as illustrated in Figure 2. These modelled clusters were then visually compared with the recorded location and magnitude data.

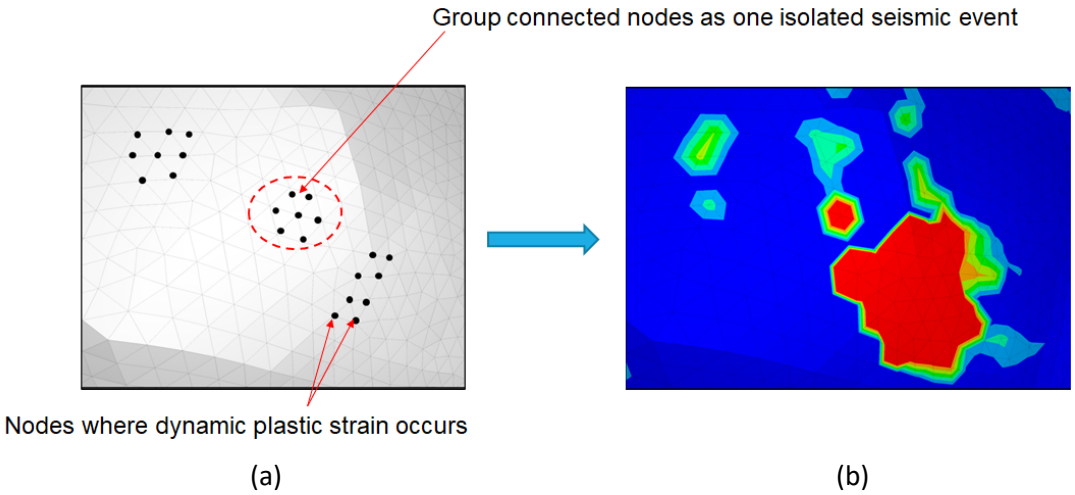

Figure 2 Calculation of seismic moment around connected nodes using Equation 1 due to plastic deformation of the zone around the specific node. (a) Position of the node; (b) Contour of calculated seismic moment)

2.3 Implementation

The first round of modelling dealt with understanding the stress field conditions only considering the lithology properties as a driver for a stress response. The output from this section of the modelling provides understanding of stress-driven failure. Client recommendations noted that it would be necessary to understand the effect of structures as well, as the cause of large seismicity has been directly attributed geological structures.

Through review of the provided geological structures, it was apparent that they all carried some form of thickness to them; therefore, it would not be appropriate to explicitly model the geological structures as interfaces taking the form of a discrete plane. Further analysis of the geological structures showed that the material present within the structures is found to be weaker than that of the containing lithology. Using these two main characteristics of the geological structures, the method of 'weak zone' was created to represent the integration of such structures within the numerical model.

As the exact properties of the geological structures are unknown, calibration was required to ensure the behaviour within the model was representative of field conditions. The calibration process underwent different trials of downgrading fault zone properties, and results were compared against historical seismicity using seismic moment and deviatoric stress. Because the IMASS constitutive model was used for the numerical modelling, the following input parameters were used to capture the rock mass response:

- GSI
    - A key parameter used to characterise the fractured rock mass
- Brittleness coefficient
    - The critical plastic shear strain serves as an indicator of the material's brittleness. It quantifies the degree to which the material exhibits brittle behaviour when subjected to shear deformation
- UCS (intact rock)
- Young's modulus (intact rock)
- mi (intact rock)
- Normal stress threshold
    - To substitute dynamic response in a static model

Understanding that the above parameters will be used as 'levers' for calibration, the modelled results from the subsequent testing are directly compared to the historical seismicity and site observations from the mine. Since this calibration is specific to understanding the response of the geological structures, it was important to ensure that the historical seismicity used for the study took into account only the seismicity that was caused by geological structures. The historical seismicity was filtered using a high Es/Ep ratio threshold greater than 10, which is representative of a fault slip event. Using the historical filtered seismicity, the cumulative seismic moment of each time step can be calculated, providing insight into the level of activity experienced throughout the years. Figure 3 shows the historical cumulative seismic moment; two points of inflection are seen at the start of 2016 and the second quarter of 2020. Between the two points of inflection, there is a constant increase in seismic moment. These trends can be used for comparison and calibration of the modelled results.

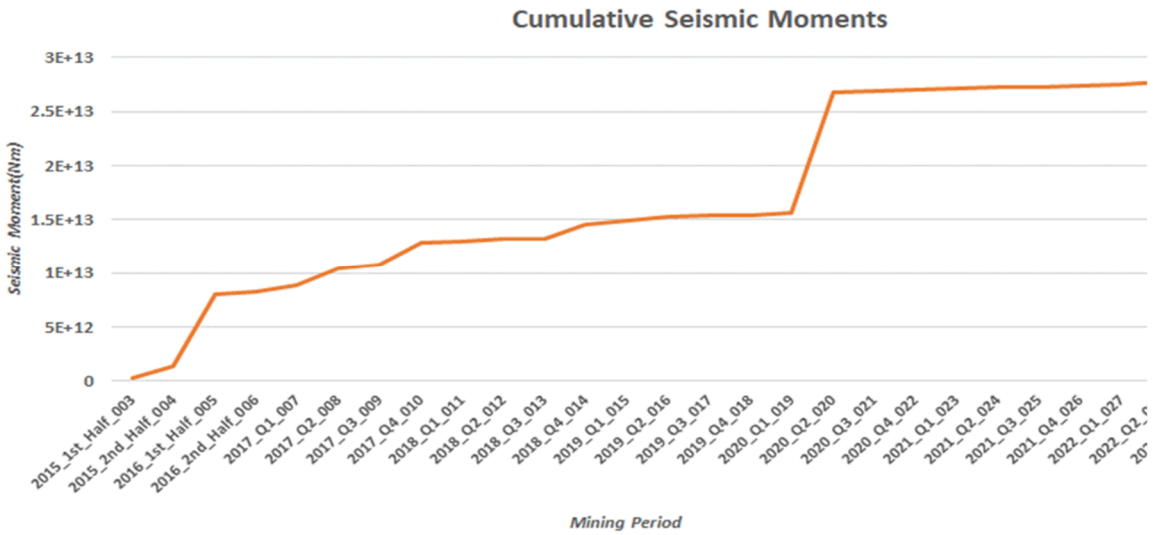

Figure 3 Historical cumulative seismic moment.

Before calibration was completed, sensitivities were modelled to understand how increasing or decreasing each parameter affects the overall seismic moment of the model result response. Instead of simply assigning values without consideration, calibration commences by conducting sensitivity analyses on GSI, brittleness coefficient, UCS, and Young's modulus (E). The parameter exhibiting the highest sensitivity is then chosen, downsized, and ultimately calibrated to best align with the calibration target. Figures 4 to 8 show the results for each sensitivity on each of the modelled results. The results are as follows:

- Critical normal stress
  - As the critical normal stress value is increased from 3 to 10, the average seismic moment for each fault decreases. This is shown in Figure 4
- GSI
  - As the GSI is scaled down between 30 to 80% of the original GSI, the average seismic moment for each fault increases. This is shown in Figure 5
- Brittleness Coefficient
  - As the brittleness coefficient scale down percentage is increased from 20 to 40% of the original value, the average seismic moment for each fault decreases. This is shown in Figure 6
- UCS
  - As the UCS scale down percentage is increased from 70 to 100% of the original UCS, the average seismic moment for each fault decreases. This is shown in Figure 7
- Young's modulus
  - As the Young's modulus scale down percentage is increased from 70 to 100% of the original Young's modulus, the average seismic moment for each fault decreases. This is shown in Figure 8

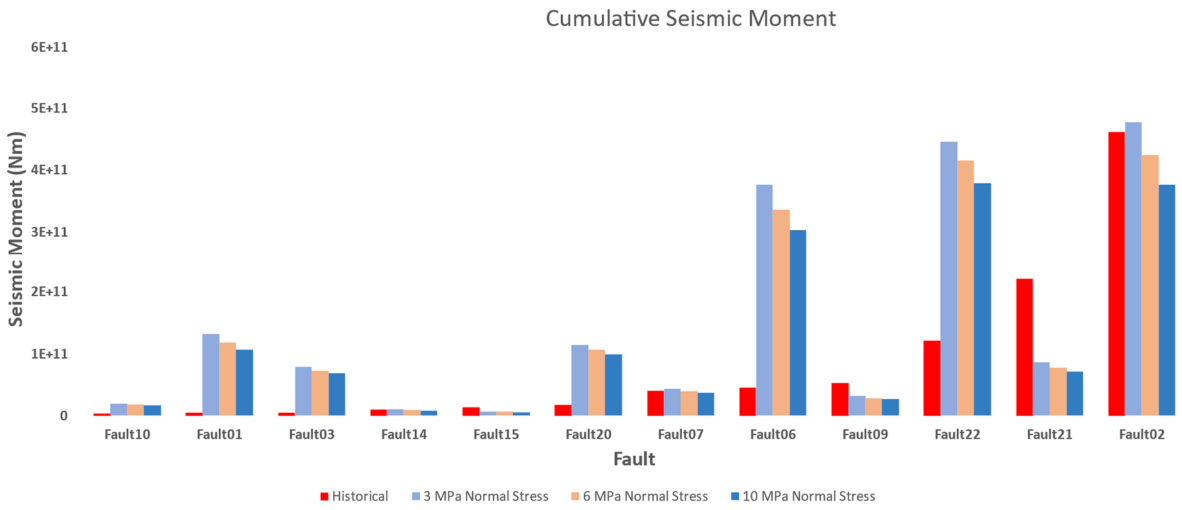

Figure 4 Critical normal stress sensitivity versus average seismic moment per fault analysed

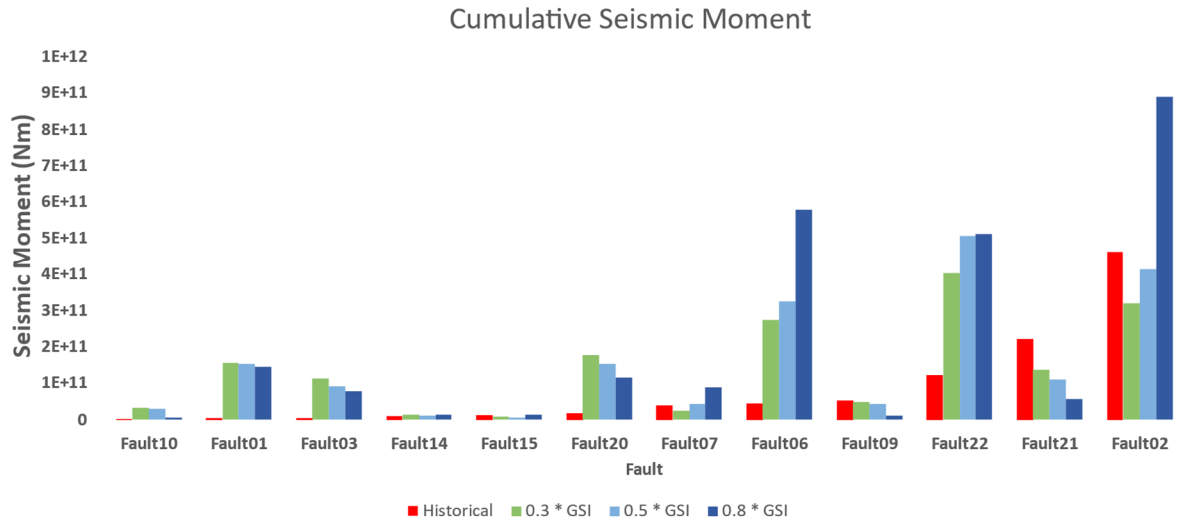

Figure 5 Geological strength index sensitivity average seismic moment per fault analysed

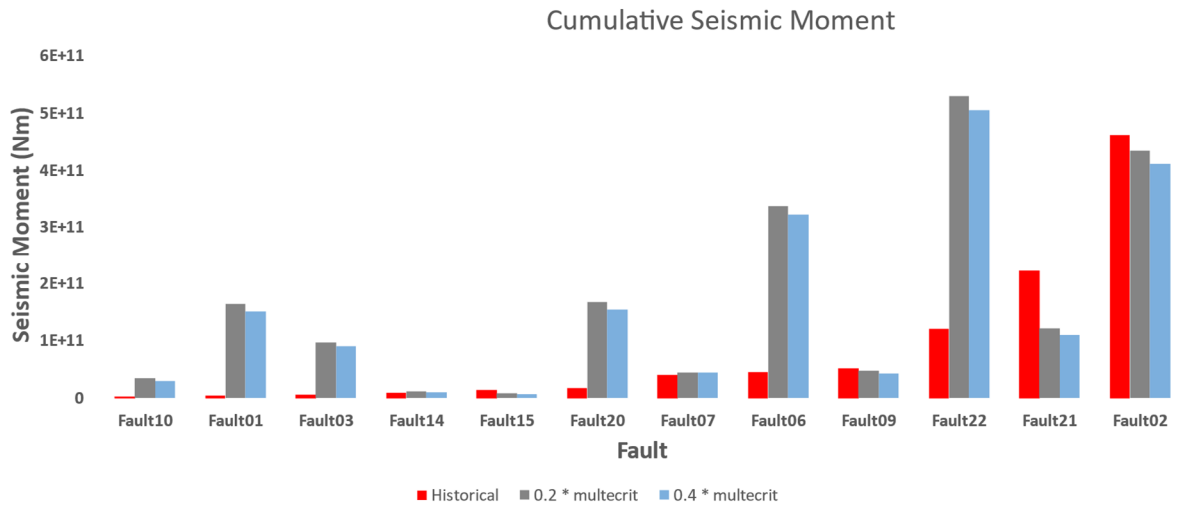

Figure 6 Brittleness coefficient sensitivity average seismic moment per fault analysed

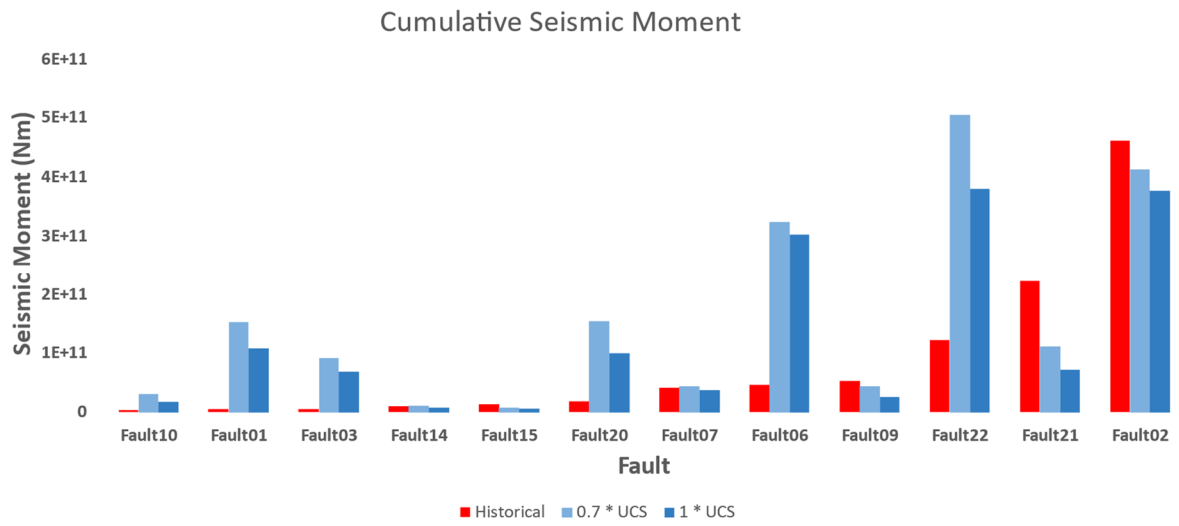

Figure 7 Uniaxial compressive strength sensitivity average seismic moment per fault analysed

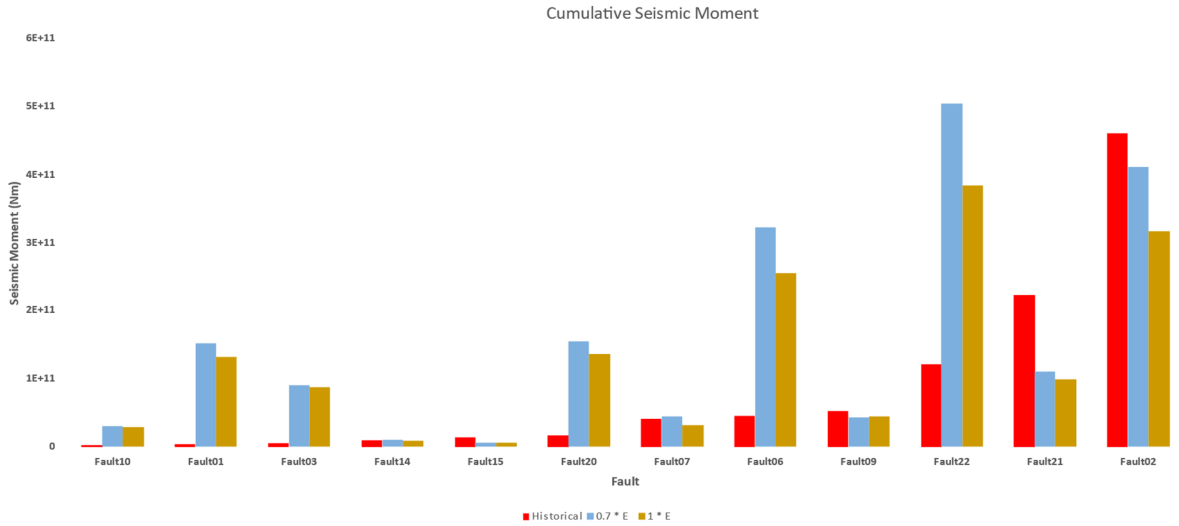

Figure 8 Young's modulus sensitivity average seismic moment per fault analysed

Using the above results, the sensitivity of each parameter can be obtained, allowing the user to understand which properties hold the most effect and adjust accordingly. The scaled properties can be increased or decreased as necessary such that the final calibrated properties are equivalent to the historical results. The cumulative seismic moment extracted from the modelled geological structures is then compared to the historical results. The overall material strength with faults will typically diminish as a result of fault movement shear stress and other environmental factors. Calibrating the model is challenging when there are multiple parameters; thus, to simplify the calibration using the sensitivity results, at the beginning, only one parameter was adjusted for calibration. The material properties within a fault zone are a result of the movement subjected within the zone, which then fractures the rock mass. The intensity of this fracturing can be quantified using GSI, and it was apparent from the sensitivity results that it also has the largest effect on the seismic moment. The final calibration properties are 80% of the host rock GSI and an assumption of 0.4 for the brittleness coefficient as the rock mass is denoted to be more ductile within the faults. UCS and Young's modulus were kept as is for their respective lithology. Figure 9 shows the comparison between the average seismic moment of each fault modelled and historically monitored. Faults that are historically deemed active and inactive correlate well overall with the modelled response. Figure 10 compares the cumulative seismic moment created by all the faults between the modelled and the historical response. In the comparison, there is a good alignment between the modelled response versus the historical response. When further analysing

the calibrated modelled response, two spikes in the cumulative seismic moment are recorded; the time frame of these two spikes may correspond to large seismic events. The modelled response captures this behaviour very well. The final calibrated model is used to analyse different sequences for the production life for potential fatal flaws and risk of large seismic events as underground operations get deeper.

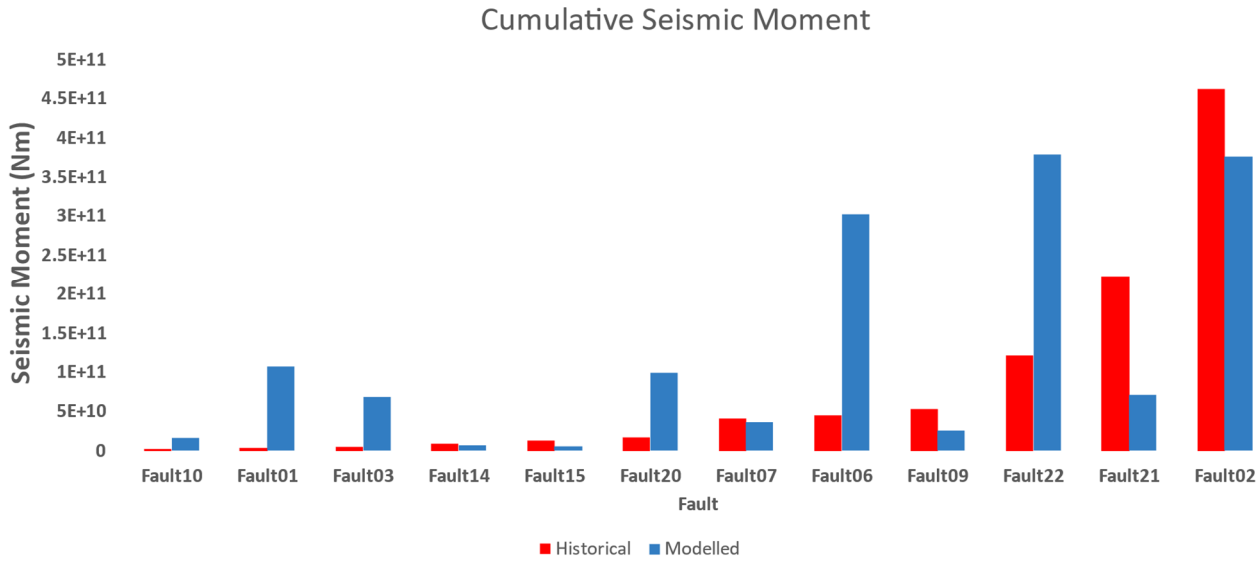

Figure 9 Modelled average seismic moment versus historical average seismic moment for each fault

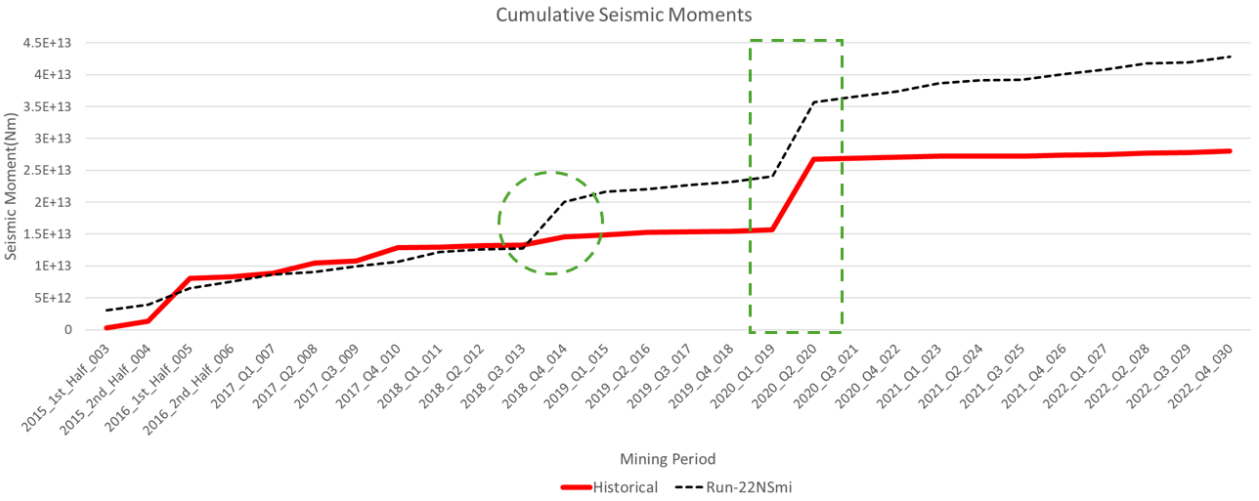

Figure 10 Modelled cumulative seismic moments versus historical cumulative seismic moments caused by fault slip

3 Conclusion

This paper explores a method by which one can estimate the seismicity induced by the potential slip of geological structures. Sites that largely attribute their high magnitude seismicity to geological structures, such as the example presented in this paper, are interested in understanding such behaviour. Analysing historical seismic events that occur at the site suggests that major structures may trigger seismic events through fault slip-induced shear movement, energy release, and stress mitigation. There have been various methodologies proposed to quantify the seismic moment caused by fault slip. In the area of interest where this study was conducted, there are a total of 22 major mapped faults, and certain significant seismic events have been linked to fault slip. To quantitatively estimate seismic events triggered by a fault slip mechanism, a

conservative assumption is made regarding energy release due to the plastic shearing of the fault. A FLAC3D model was employed to calculate plastic shear strain and normal stress in each fault zone, with the seismic moment derived from the sum of released energy in connected zones. Calibration of fault properties against historical seismicity is essential before utilising the model for predictive simulations. The calibrated model that included geological structures will be used to assess multiple production sequences for risk relating to large seismic events. This comprehensive approach offers valuable insight into identifying and mitigating stress hazards that can be used in other deep mining operations that attribute their geological structures as a major source for seismicity.

References

Andrieux, P, Zhu, H, Labrie, D, Doucet, C, Lampron, S & Fleury, D 2004, 'Determination and validation of the rock mass postpeak mechanical properties for a 3DEC strain-softening model of the 680 sill pillar at Louvicourt mine', *Proceedings First International Symposium on UDEC/3DEC*, Bochum.

Basson, G, Bassom, PA & Salmon, B 2021, 'Simulating mining-induced seismicity using the material point method', *Rock Mechanics and Rock Engineering*, vol. 54.

Blanksma, D, Hazzard, J, Damjanac, B, Lam, T & Hoessein, A.K 2022, 'Effect of fault reactivation on deformation of off-fault fractures near a generic deep geological repository in crystalline rock in Canada', *Rock Mechanics and Rock Engineering,* vol. 26, no. 1.

Board, M 1996, 'Numerical examination of mining-induced seismicity', *Proceedings Eurock '96, Prediction and Performance in Rock Mechanics and Rock Engineering*, Routledge, London.

Cancino, C, Garza-Cruz, T & Pierce, M 2019, *Assessment of Potential for Caving-Induced Fault Slip Seismicity at Resolution Copper Mine*, ITASCA, Minneapolis.

Cotesta, L, O'Connor, C, Brummer, RK, Punkkinen, AR 2014, 'Numerical Modelling and Scientific Visualization-Integration of Geomechanics into Modern Mine Designs', M Hudyma and Y Potvin (Eds*). Deep Mining 2014. Proceedings of the Seventh International Conference on Deep and High Stress Mining,* Australian Centre for Geomechanics, Perth, pp. 377–394, https://doi.org/10.36487/ACG_rep/1410_25_Cotesta

ITASCA 2023, *FLAC3D 9.0*, computer software, Minneapolis, https://docs.itascacg.com/itasca910/flac3d/docproject/source/flac3dhome.html

Katsaga, T & Pierce, ME 2013, 'Continuous monitoring of synthetic seismicity: slip on joints', *Proceedings of the 47th US Rock Mechanics/Geomechanics Symposium*, American Rock Mechanics Association, Alexandria.

Martin, CD 1993, *The Strength of Massive Lac du Bonnet Granite Around Underground Openings*, PhD thesis, University of Manitoba, Manitoba.

Mercer, R & Bawden, WF 2005, 'A statistical approach for the integrated analysis of mine-induced seismicity and numerical stress estimates, a case study—Part I: developing the relations', *International Journal of Rock Mechanics and Mining Sciences*, vol. 42, no. 1, pp. 47–72.

Ryder, JA 1987, 'Excess shear stress (ESS): An engineering criterion for assessing unstable slip and associated rockburst hazards', *Proceedings Sixth International Congress on Rock Mechanic*s, International Society for Rock Mechanics, Lisbon.

Ryder, JA 1988, 'Excess shear stress in the assessment of geologically hazardous situations', *Journal of the South African Institute of Mining and Metallurgy*, vol. 88, no. 1, pp. 27–39.

Salamon, MDG 1993, 'Some applications of geomechanical modelling in rockburst and related research', in P Young (ed.), P*roceedings of the 3rd International Symposium on Rockbursts and Seismicity in Mines*, A.A. Balkema, Rotterdam, pp. 297–309.

Sjöberg, J, Perman, F, Quinteiro, C, Malmgren, L, Dahnér-Lindkvist, C & Boskovic, M 2012, 'Numerical analysis of alternative mining sequences to minimise the potential for fault slip rockbursting', in Y Potvin (ed.), *Deep Mining 2012: Proceedings of the Sixth International Seminar on Deep and High Stress Mining*, Australian Centre for Geomechanics, Perth, pp. 357–372, https://doi.org/10.36487/ACG_rep/1201_26_sjoberg